

Phonon-induced lifetime broadenings of electronic states and critical points in Si and Ge

P. Lautenschlager, P. B. Allen,* and M. Cardona

*Max-Planck-Institut für Festkörperforschung, Heisenbergstrasse 1, D-7000 Stuttgart 80,
Federal Republic of Germany*

(Received 1 November 1985)

We present calculations of the lifetime broadenings of electronic states produced by the electron-phonon interaction in semiconductors and of their dependence on temperature. This effect is evaluated as a complex self-energy of the electronic states. The real part of this self-energy describes a shift of the bands with temperature, whereas the imaginary part is responsible for the broadening of the states. For the calculations based on perturbation theory to second order in atomic displacement we use a local pseudopotential with a basis of 59 plane waves, the lattice dynamics of Weber's bond-charge model, and a tetrahedron method for doubly constrained Brillouin-zone integrals. Results are given for points along the Λ and Δ direction of the Brillouin zone for Si and Ge, thus obtaining the temperature dependence of the broadening parameters of the interband critical points E_0 , E'_0 , E_1 , and E_2 . The results are compared with experimental data obtained from ellipsometric measurements of the temperature dependence of the dielectric function. Remarkable agreement between calculated and measured data is found.

I. INTRODUCTION

With increasing temperature semiconductors show a shift in the energy of electronic states and an increasing lifetime broadening. These effects can be investigated by measuring structures in the optical spectra, such as those obtained by absorption or ellipsometric techniques.¹ In the case of germanium and silicon such spectra reveal an indirect absorption edge, not considered here since its broadening is small, and other edges or critical points (CP's) labeled E_0 , E'_0 , E_1 , E_2, \dots .² The E_0 edge is the lowest direct edge of Ge and corresponds to transitions at the Γ point of the Brillouin zone (BZ). The E_1 edge corresponds to transitions from the highest valence band to the lowest conduction band along the $\langle 111 \rangle$ directions; for Si it is nearly degenerate with the E'_0 gap which occurs at Γ . The E_2 transitions correspond to electronic states not well localized in \mathbf{k} space which include or are close in energy to the lowest gap at the X point.

While quantitative data for the shifts of energy gaps and critical points with temperature are very abundant, especially for Ge and Si,²⁻⁷ the corresponding data for broadenings are less abundant. Systematic data versus temperature have recently been obtained for a number of materials [Si (Refs. 3 and 7), Ge (Ref. 4), InSb (Ref. 5), and α -Sn (Ref. 6)]. In Refs. 3-7 the shift and the broadening of the E_0 , E'_0 , E_1 , and E_2 gaps, and also the $E_1 + \Delta_1$ gap which is split from E_1 by spin-orbit interaction, is investigated. The broadenings obtained and their temperature dependence are analyzed in a phenomenological manner. We present here a microscopic analysis of these broadenings for Ge and Si.

Electrons high up in the conduction bands and holes deep into the valence band can decay into electronic excitations through Coulomb interaction. This decay is of the Auger type.⁸ The resulting lifetime broadenings are very small unless the energies of electrons (holes) with respect

to the band edge become close to the plasma frequency (16 eV). Up to ~ 3 eV, for instance, the broadening due to this kind of decay is less than 10 meV.⁸ The broadenings observed for the E_0 , E_1 , E'_0 , and E_2 edges, have initial- and final-state energies which are less than 3 eV from the band edge. Their lifetime broadenings⁴⁻⁷ are more than 10 meV and they are temperature dependent. Since the Auger processes should be nearly independent of temperature, the observed broadenings must be due to electron-phonon interaction. In the presence of this interaction the electrons (holes) become quasiparticles with a temperature-dependent self-energy. The real part of this self-energy corresponds to an energy shift of the optical gaps, its imaginary part to a lifetime broadening.

Theoretical work so far has concentrated on the calculation of the temperature-dependent energy shift of electronic states produced by the electron-phonon interaction. Two different contributions to this shift arise:⁹ that of thermal expansion and the direct renormalization of band energies by electron-phonon interactions. The first contribution can easily be calculated from the presumably known dependence of the band structure on volume, together with the expansion coefficients. Theoretical interest has thus focused on the effect of the electron-phonon interaction. This effect can, in turn, also be broken up into two contributions: the Debye-Waller terms¹⁰ and the Fan^{11,12} or "self-energy" terms. Both terms are obtained from a perturbative calculation¹³ of the electron self-energy to second order in atomic displacement \mathbf{u} . The corresponding Feynman diagrams are shown in Fig. 1. The Debye-Waller correction is an effect of the second-order electron-phonon interaction taken to first order in perturbation theory and depends only on phonon amplitude and not otherwise on the particular phonon involved. The "self-energy" contributions, which are different for each electronic state and also for each phonon involved, arise from the first-order electron-phonon in-

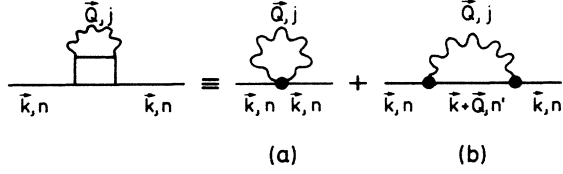


FIG. 1. Self-energy graphs which give the temperature renormalization of the bands to second order in the displacement \mathbf{u} . (a) represents the Fan terms; (b) the lowest-order Debye-Waller correction.

teraction taken to second order in perturbation theory. These two corrections are related by a sum rule derived from translational invariance.¹³ It has been shown that both Fan and Debye-Waller terms should be included in the calculations of the temperature shift of the band structure¹³⁻¹⁵ so as to preserve translational invariance^{13,16} and to obtain a good description of the experimental data.¹⁴

The temperature shifts of the lowest direct gaps at the Γ point of Si and Ge (Refs. 17 and 18) have been calculated. These calculations have been extended recently to electronic states at other points of the BZ,¹⁹ thus obtaining the temperature shifts of the indirect gaps, of the second-lowest direct gap, and of the E_1 and E_2 CP's. The agreement with experimental data is excellent, except for the E_2 CP, a shortcoming which may partly result from the uncertainties in the location of the E_2 transitions in \mathbf{k} space.

Realistic calculations of the temperature-dependent broadenings of electronic states in semiconductors are, to our knowledge, limited to a study by Lawaetz of the broadening of the $E_0 + \Delta_0$ edge of tetrahedral semiconductors, split from E_0 by spin-orbit interaction.²⁰ This author analyzed optical-absorption data near $E_0 + \Delta_0$ and obtained from them the interaction coefficient (deformation potential) between holes at Γ and optical phonons.

We present in this paper a calculation of the broadening of the electronic states which contribute to the E_0 , E'_0 , E_1 , and E_2 gaps of Ge and Si. The calculation is based on the empirical pseudopotential band structure of these materials²¹ and the lattice dynamics of Weber.²² These broadenings are obtained by evaluating the imaginary part of the corresponding self-energy (Fan terms) with the rigid-ion model for the potential of the distorted lattice. The results are found to be in excellent agreement with experimental data.

II. THEORY

In deriving the relevant relations for the phonon-induced broadening we follow the theory of Refs. 13 and 17. Consider a crystal with atoms of species κ which occupy sites $\mathbf{R}(l, \kappa)$ and have displacements $\mathbf{u}(l, \kappa)$ from equilibrium, where l labels the unit cells. In order to describe the renormalization of the semiconductor band structure by the electron-phonon interaction, the electron-atom interaction $V(\mathbf{r} - \mathbf{R}(l, \kappa) - \mathbf{u}(l, \kappa))$ is Taylor

expanded about the positions $\mathbf{u}(l, \kappa) = 0$. The zeroth-order Hamiltonian H_0 gives the one-electron states $|\mathbf{k}, n\rangle$ and band energies $\epsilon_{\mathbf{k}n}$ where (\mathbf{k}, n) are wave-vector and band index. The first two terms of the expansion of $V(\mathbf{r} - \mathbf{R}(l, \kappa) - \mathbf{u}(l, \kappa))$ in powers of $\mathbf{u}(l, \kappa)$ are¹³

$$H_1 = \sum_{l, \kappa} \frac{\partial V}{\partial R_\alpha(l, \kappa)} u_\alpha(l, \kappa), \quad (1)$$

$$H_2 = \frac{1}{2} \sum_{l, \kappa, l', \kappa'} \frac{\partial^2 V}{\partial R_\alpha(l, \kappa) \partial R_\beta(l', \kappa')} u_\alpha(l, \kappa) u_\beta(l', \kappa'). \quad (2)$$

The subscripts α, β denote Cartesian components which are summed when repeated. The adiabatic approximation allows the neglect of time dependence of $\mathbf{u}(l, \kappa)$. To second order in $\mathbf{u}(l, \kappa)$ we obtain, using standard Rayleigh-Schrödinger perturbation theory,¹³

$$\begin{aligned} E_{\mathbf{k}n}(\{\mathbf{u}(l, \kappa)\}) &= \epsilon_{\mathbf{k}n} + \langle \mathbf{k}, n | (H_1 + H_2) | \mathbf{k}, n \rangle \\ &+ \sum'_{\mathbf{k}', n'} \frac{|\langle \mathbf{k}', n' | H_1 | \mathbf{k}, n \rangle|^2}{\epsilon_{\mathbf{k}n} - \epsilon_{\mathbf{k}'n'} + i\eta} \\ &= \epsilon_{\mathbf{k}n} + \Sigma^{\text{DW}} + \Sigma^{\text{SE}}. \end{aligned} \quad (3)$$

The prime on the summation indicates that the term $(\mathbf{k}', n') = (\mathbf{k}, n)$ is omitted. The first correction term to the unperturbed energy of the initial state $\epsilon_{\mathbf{k}n}$, Σ^{DW} , is purely real (Debye-Waller term) whereas in the second correction term, the "self-energy" term, Σ^{SE} , every state is endowed with a complex self-energy. Equation (3) has been derived with standard Rayleigh-Schrödinger perturbation theory, which implies that the phonon frequencies are small compared with the relevant scale of electronic energies (typically the density of electronic states does not vary appreciably in less than 0.1 eV). This approximation should be good enough for our purposes. The resulting equations can easily be generalized to include finite phonon frequencies using standard many-body perturbation technique.¹⁵

Equation (3) is closely analogous to the standard calculation of the effects of impurities on band structure. Just as in the impurity case, the final step is to perform an ensemble average (in our case, mimicking a time average) over the thermal displacements $\mathbf{u}(l, \kappa)$. The result is written as

$$E_{\mathbf{k}n}(T) = \epsilon_{\mathbf{k}n} + \Delta_{\mathbf{k}n}^{\text{DW}} + \Delta_{\mathbf{k}n}^{\text{SE}} + \frac{i}{2\tau_{\mathbf{k}n}}. \quad (4)$$

$\Delta_{\mathbf{k}n}$ is the shift of the band structure induced by the Debye-Waller term (DW) and the self-energy term (SE) and $\tau_{\mathbf{k}n}$ is a lifetime. The temperature shift has been calculated in previous papers,¹⁷⁻¹⁹ hence we focus our attention on the evaluation of the imaginary part of $E_{\mathbf{k}n}$, connected with the lifetime $\tau_{\mathbf{k}n}$. The last term of Eq. (3) can be rewritten after ensemble averaging as

$$\Sigma_{\mathbf{k}n}^{\text{SE}} = \lim_{\eta \rightarrow 0^+} \int \frac{dE'}{E - E' + i\eta} B_{\mathbf{k}n}(E'), \quad (5)$$

where $B_{\mathbf{k}n}(E)$ are the matrix elements of the spectral electron-phonon operator which are defined as

$$B_{\mathbf{k}n}(E) = \sum_{\mathbf{k}',n'} \langle \langle \mathbf{k},n | H_1 | \mathbf{k}',n' \rangle \langle \mathbf{k}',n' | H_1 | \mathbf{k},n \rangle \rangle \times \delta(E - \varepsilon_{\mathbf{k}',n'}) . \quad (6)$$

The outer brackets denote the thermal average. Using the Dirac identity, Eq. (5) can be written

$$\Sigma_{\mathbf{k}n}^{\text{SE}}(E) = P \int \frac{B_{\mathbf{k}n}(E')}{E - E'} dE' - i\pi B_{\mathbf{k}n}(E) , \quad (7)$$

where P means the principal value. In this way we obtain the real and imaginary part of the self-energy term

$$\begin{aligned} \partial \Gamma_{\mathbf{k}n} / \partial n_{\mathbf{Q}j} = & \frac{\pi}{N} \sum_{\kappa, \kappa', n'} [\langle \mathbf{k},n | \partial V / \partial R_{\alpha}(\kappa) | \mathbf{k} + \mathbf{Q},n' \rangle \langle \mathbf{k} + \mathbf{Q},n' | \partial V / \partial R_{\beta}(\kappa') | \mathbf{k},n \rangle] e^{-i\mathbf{Q} \cdot (\boldsymbol{\tau}_{\kappa} - \boldsymbol{\tau}_{\kappa'})} \\ & \times \hbar (M_{\kappa} M_{\kappa'} \omega_{\mathbf{Q}j}^2)^{-1/2} \varepsilon_{\alpha}(-\mathbf{Q},j;\kappa) \varepsilon_{\beta}(\mathbf{Q},j;\kappa') \delta(\varepsilon_{\mathbf{k}n} - \varepsilon_{\mathbf{k}+\mathbf{Q},n'}) . \end{aligned} \quad (11)$$

To derive this result, Bloch's theorem has been used and the same conventions as in Ref. 17: M_{κ} is the mass of the κ th atom in the unit cell at position $\boldsymbol{\tau}_{\kappa}$, N the number of unit cells in the crystal, $\varepsilon_{\alpha}(\mathbf{Q},j;\kappa)$ are the polarization vectors of the phonons obtained by solving the lattice dynamical problem with some appropriate model.²² Equation (11) shows that only phonons which couple to an electronic state with the same energy $\varepsilon_{\mathbf{k}+\mathbf{Q},n'}$ as the initial state $\varepsilon_{\mathbf{k}n}$ can make a contribution to $\Gamma_{\mathbf{k}n}(T)$ (real transitions). In a full nonadiabatic calculation, the δ function would become $\delta(\varepsilon_{\mathbf{k}n} - \varepsilon_{\mathbf{k}+\mathbf{Q},n} \pm \omega_{\mathbf{Q}j})$, but this correction has negligible significance except for states at the extreme top or bottom of a band where the broadening is nevertheless very small.

We now apply the results given above to the diamond structure with the origin of the unit cell chosen to be such

$$\partial \Gamma_{\mathbf{k}n} / \partial n_{\mathbf{Q}j} = \frac{\pi}{2} \sum_{n'} [\Gamma(\mathbf{k},n,n';\mathbf{Q}) \cdot \mathbf{u}(\mathbf{Q},j;+) + \Theta(\mathbf{k},n,n';\mathbf{Q}) \cdot \mathbf{u}(\mathbf{Q},j;-)]^2 \delta(\varepsilon_{\mathbf{k}n} - \varepsilon_{\mathbf{k}+\mathbf{Q},n'}) . \quad (13)$$

The displacements $\mathbf{u}(\mathbf{Q},j,\pm)$ are the even and odd combinations of displacement of the two atoms in the unit cell which are obtained from the phonon eigenvectors.¹⁷ We have obtained these eigenvectors with Weber's bond-charge model.²² The β th component of Γ was evaluated to be¹⁷

$$\begin{aligned} \Gamma_{\beta}(\mathbf{k},n,n';\mathbf{Q}) \equiv & \sum_{\mathbf{G},\mathbf{G}'} c_{\mathbf{k}+\mathbf{Q},n'}(\mathbf{G}') c_{\mathbf{k}n}(\mathbf{G}) (\mathbf{G}' - \mathbf{G} + \mathbf{Q})_{\beta} \\ & \times V(\mathbf{G}' - \mathbf{G} + \mathbf{Q}) \cos[(\mathbf{G}' - \mathbf{G}) \cdot \boldsymbol{\tau}] . \end{aligned} \quad (14)$$

The expression for Θ_{β} is the same as that for Γ_{β} , except that the cosine is replaced by the sine. Because of the δ function in Eq. (13), the broadenings are expected to be roughly proportional to the electronic density of states at the energy of the initial state.

$$\Delta_{\mathbf{k}n}^{\text{SE}} = \text{Re} \Sigma_{\mathbf{k}n}^{\text{SE}}(\varepsilon_{\mathbf{k}n}) = P \int \frac{B_{\mathbf{k}n}(E')}{\varepsilon_{\mathbf{k}n} - E'} dE' , \quad (8)$$

$$\Gamma_{\mathbf{k}n} = \frac{1}{2\tau_{\mathbf{k}n}} = -\text{Im} \Sigma_{\mathbf{k}n}^{\text{SE}}(\varepsilon_{\mathbf{k}n}) = \pi B_{\mathbf{k}n}(\varepsilon_{\mathbf{k}n}) . \quad (9)$$

Writing more explicitly with the use of Eqs. (1) and (6), Eq. (9) is

$$\Gamma_{\mathbf{k}n}(T) = \sum_{\mathbf{Q},j} \partial \Gamma_{\mathbf{k}n} / \partial n_{\mathbf{Q}j} (n_{\mathbf{Q}j} + \frac{1}{2}) , \quad (10)$$

where $n_{\mathbf{Q}j}$ is the Bose-Einstein occupation factor $(e^{\beta\omega_{\mathbf{Q}j}} - 1)^{-1}$ for the phonon mode (\mathbf{Q},j) of energy $\omega_{\mathbf{Q}j}$. The coefficient $\partial \Gamma_{\mathbf{k}n} / \partial n_{\mathbf{Q}j}$ is given by

that $\boldsymbol{\tau} = \boldsymbol{\tau}_1 = -\boldsymbol{\tau}_2 = (1,1,1)a/8$ (midway between two nearest-neighbor atoms). The electron energies $\varepsilon_{\mathbf{k}n}$ and wave functions $\psi_{\mathbf{k}n}$ are given by solving the secular equation

$$\begin{aligned} 0 = & \sum_{\mathbf{G}'} \{ [(\mathbf{k} + \mathbf{G}')^2 - \varepsilon_{\mathbf{k}n}] \delta_{\mathbf{G}\mathbf{G}'} \\ & + V(\mathbf{G} - \mathbf{G}') S(\mathbf{G} - \mathbf{G}') \} c_{\mathbf{k}n}(\mathbf{G}') , \\ \psi_{\mathbf{k}n} = & \Omega_c^{-1/2} \sum_{\mathbf{G}} c_{\mathbf{k}n}(\mathbf{G}) e^{i(\mathbf{k} + \mathbf{G}) \cdot \boldsymbol{\tau}} , \\ \sum_{\mathbf{G}} & |c_{\mathbf{k}n}(\mathbf{G})|^2 = 1 , \end{aligned} \quad (12)$$

where $V(\mathbf{G})$ is the local pseudopotential form factor and $S(\mathbf{G})$ the structure factor $\cos(\mathbf{G} \cdot \boldsymbol{\tau})$. Equation (11) can be written in the form convenient for numerical calculations:

III. NUMERICAL PROCEDURE

Our aim is the evaluation of the temperature dependence of the phonon-induced lifetime broadening $\Gamma_{\mathbf{k}n}(T)$, given by Eq. (10). We rewrite this equation as

$$\Gamma_{\mathbf{k}n}(T) = \int_0^{\infty} d\Omega g^2 B(\mathbf{k},n;\Omega) [n_{\mathbf{Q}j}(T) + \frac{1}{2}] , \quad (15)$$

$$g^2 B(\mathbf{k},n,\Omega) \equiv \pi \sum_{\mathbf{Q},j} \partial \Gamma_{\mathbf{k}n} / \partial n_{\mathbf{Q}j} \delta(\Omega - \omega_{\mathbf{Q}j}) . \quad (16)$$

In Eq. (16) we have introduced a temperature-independent electron-phonon spectral function $g^2 B(\mathbf{k},n,\Omega)$ similar to $g^2 F(\mathbf{k},n,\Omega)$ used for the temperature shift of the gap in Refs. 17–19. The function $g^2 B$ corresponds to the density of phonon states weighed by electron-phonon matrix elements.

The first step of our procedure is to calculate the spectral function $g^2 B$ and then to perform the integral over

the phonon frequencies Ω with the Bose-Einstein occupation factor in order to obtain the temperature dependence of $\Gamma_{\mathbf{k}n}$. For calculating g^2B we must perform a summation over the BZ with two δ functions of the kind

$$g^2B(\mathbf{k}, n; \Omega) = \sum_{\mathbf{Q}, j} W(\mathbf{k}, n; \mathbf{Q}, j) \delta(\epsilon_{\mathbf{k}+\mathbf{Q}, n'} - \epsilon_{\mathbf{k}n}) \times \delta(\Omega - \omega_{\mathbf{Q}, j}). \quad (17)$$

Such a summation is constrained to the intersection of two different constant-energy surfaces, one which corresponds to electronic energy differences and the other to phonon energies.

Allen²³ has generalized the tetrahedron method to such doubly constrained BZ summations.²⁴ Simple analytic results have been obtained by linearly interpolating the energies and weight functions throughout a small tetrahedron.²³

We have used this tetrahedron method to compute the spectral function $g^2B(\mathbf{k}, n; \Omega)$. The irreducible $\frac{1}{48}$ th wedge of the BZ was divided into 228 small tetrahedra which correspond to a discrete mesh of 89 \mathbf{k} points. As in the calculations of the energy shifts with temperature,¹⁷⁻¹⁹ the bond-charge-model²² programs²⁵ of Weber were used. The band structure was calculated from Eq. (12) using the local pseudopotential form factors from Cohen and Bergstresser.²¹ For the $V(\mathbf{Q})$ in Eq. (14), with \mathbf{Q} not equal to a reciprocal-lattice vector \mathbf{G} , we used the interpolation and the extrapolation to $V(\mathbf{0}) = -2\epsilon_F/3$, shown in Fig. 1 of Ref. 18.

For an initial \mathbf{k} state at the Γ point the \mathbf{Q} sum in Eq. (17) can be restricted to the irreducible wedge of the BZ. For a general \mathbf{k} point the sum can also be carried out over the irreducible part of the BZ, then adding similar contributions from all vectors in the star of \mathbf{k} so as to obtain g^2B . For a \mathbf{k} point along the Λ line this means that the \mathbf{Q} sum in Eq. (17) must be carried out in the $\frac{1}{48}$ th wedge of the BZ for the eight points of the star of $|\mathbf{k}|[1,1,1]$. In this way it is possible to determine the temperature dependence of the lifetime broadening $\Gamma_{\mathbf{k}n}(T)$ of every electronic state in the BZ. We have calculated $\Gamma_{\mathbf{k}n}(T)$ for the following transitions in Si and Ge: the direct transitions at the Γ point, the E_1 and E_2 CP's, and the transitions along the Δ line. The E_1 transitions take place between the Λ_3 valence band (VB) and the Λ_1 conduction band (CB) between

$$(2\pi/a) \langle \frac{1}{4}, \frac{1}{4}, \frac{1}{4} \rangle$$

and

$$(2\pi/a) \langle \frac{1}{2}, \frac{1}{2}, \frac{1}{2} \rangle.$$

The region for the E_2 transitions is not well defined. We have used the points $(2\pi/a)(0.9, 0.1, 0.1)$ for Si and $(2\pi/a)(\frac{3}{4}, \frac{1}{4}, \frac{1}{4})$ for Ge as representative points.²⁶ The calculations must be carried out separately in each case for the conduction- and the valence-band states. The states at the absolute maximum of the VB ($\Gamma_{25'}$) and at the absolute minimum of the CB ($0.85X_1$ in Si and L_1 in Ge), do not show any phonon-induced broadening since there are no other electronic states with the same energy.

This is the consequence of the assumption of negligible phonon frequency. If this assumption were lifted band-edge states would broaden slightly through phonon absorption, i.e., at $T \neq 0$.

IV. RESULTS

In Figs. 2 and 3 we show as an example the calculated spectral functions $g^2B(\Omega)$ for initial states along the Λ direction of Si, including those at the Γ and L points. Figure 2 indicates that for the highest VB states the leading contribution to the broadening is due to the optical phonons and increases with increasing separation from Γ . Near the Γ point there is nearly no contribution from acoustic phonons, close to the L point small structure related to acoustic phonons near the edge of the BZ is seen. The total area under $g^2B(\Omega)$ increases with increasing separation from the Γ point because of the increasing electronic density of states. The corresponding sequence of spectral functions for the lowest CB of Si can be seen in Fig. 3. Here the area under $g^2B(\Omega)$ decreases with increasing separation from the Γ point. The structure at about 20 meV indicates that the transverse acoustic phonons, having a flat dispersion near the X point, contribute

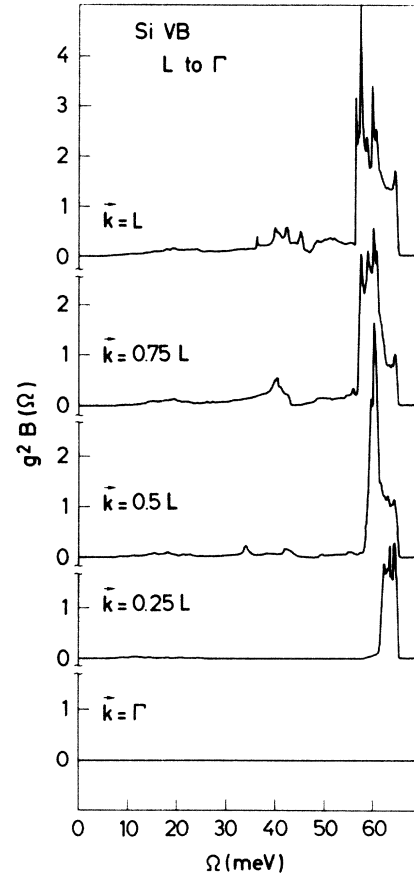


FIG. 2. Dimensionless spectral functions $g^2B(\Omega)$ for the highest valence-band state (VB) of Si. A sequence of \mathbf{k} points from L to Γ is shown.

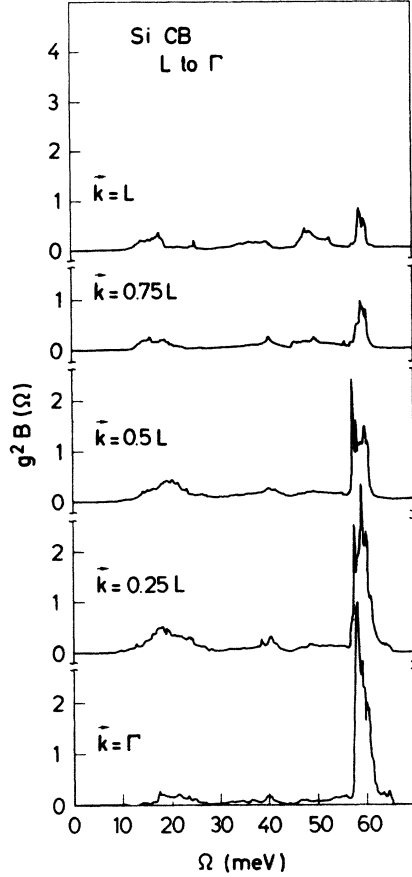


FIG. 3. Dimensionless spectral functions $g^2B(\Omega)$ for the lowest conduction-band state (CB) of Si. A sequence of points from L to Γ is shown.

strongly to the broadening of the CB states in contrast to the case of VB states.

Figures 4 and 5 show the temperature dependence of the broadening of electronic states along the Λ direction for the VB (lower part of figures) and the CB (upper part) for Si and Ge, respectively. In Figs. 6 and 7 we display the broadenings along the Δ line of Si and Ge, again for the electronic states in the highest VB and lowest CB, including also the broadening of two representative states contributing to the E_2 transition $[(0.9,0.1,0.1)$ for Si and $(0.75,0.25,0.25)$ for Ge, in units of $2\pi/a$]. The zero-point broadening $\Gamma(0)$ is proportional to the area under $g^2B(\Omega)$. In the high-temperature limit there is a factor of $2k_B T/\hbar\Omega$ in the integrand which gives more weight to the low-frequency phonons. Hence, a broadening strongly increasing with T indicates a considerable contribution from acoustic phonons.

In previous works⁴⁻⁶ experimental data for the temperature dependence of the broadening of the CP's were fitted with a phenomenological expression based on the Bose-Einstein statistical factor which should take into account electron-phonon interactions with phonons of average frequency $k_B\Theta/\hbar$:⁴

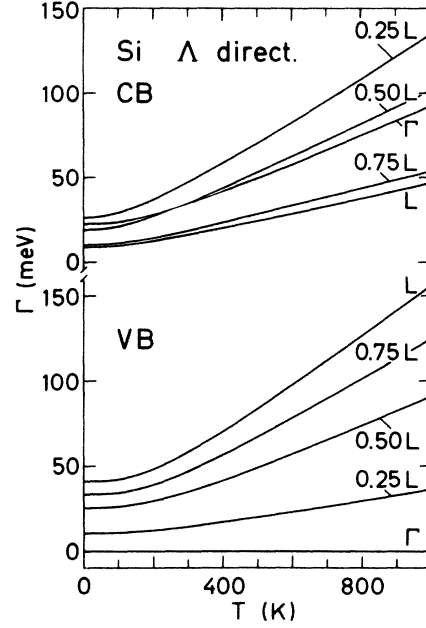


FIG. 4. Temperature dependence of the broadening Γ_{kn} of valence-band (VB), and conduction-band (CB) states of Si along the Λ direction of the Brillouin zone.

$$\Gamma(T) = \Gamma_0 \left[1 + \frac{2}{e^{\Theta/T} - 1} \right] + \Gamma_1. \quad (18)$$

Within the present theoretical treatment Eq. (18) can only be rigorously justified if a group of phonons of frequencies close to $k_B\Theta/\hbar$ yield the dominant contribution

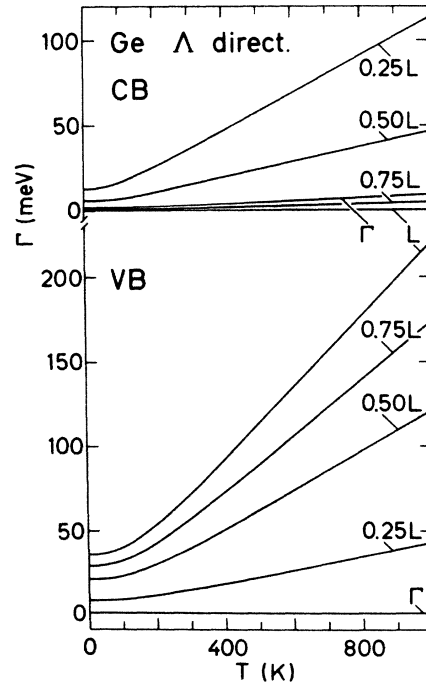


FIG. 5. Temperature dependence of the broadening Γ_{kn} of valence-band (VB) and conduction-band (CB) states of Ge along the Λ direction of the Brillouin zone.

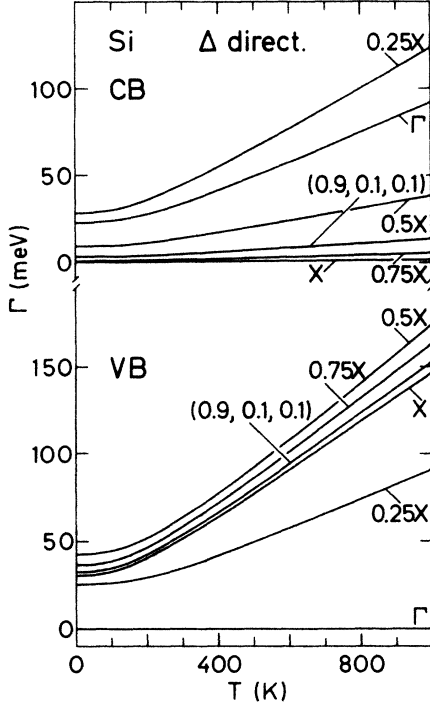


FIG. 6. Temperature dependence of the broadening Γ_{kn} of valence-band (VB) and conduction-band (CB) states of Si along the Δ direction of the Brillouin zone. The result for the representative point for the E_2 transitions $(2\pi/a)(0.9, 0.1, 0.1)$ is also included.

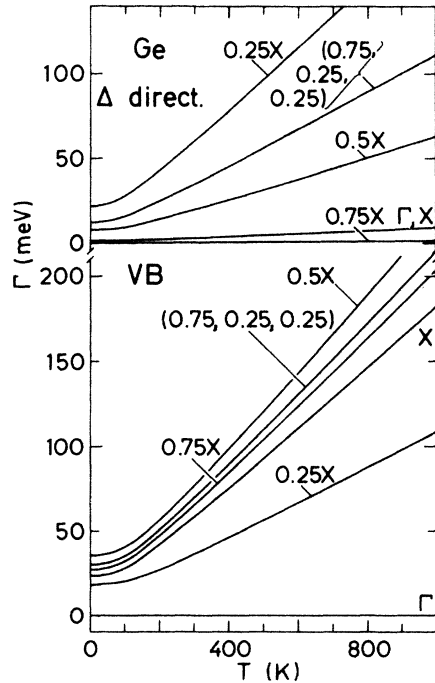


FIG. 7. Temperature dependence of the broadening Γ_{kn} of valence-band (VB) and conduction-band (CB) states of Ge along the Δ direction of the Brillouin zone. The result for the representative point for the E_2 transitions $(2\pi/a)(0.75, 0.25, 0.25)$ is also included.

to $\Gamma(T)$. Figures 2 and 3 suggest that this is usually the case for the TO phonons except at very low temperatures. In view of the success of Eq. (18) in fitting experimental data, and of its simplicity, we have attempted to use it here to fit the calculated $\Gamma(T)$. By taking into account all three parameters (Γ_0 , Γ_1 , and Θ), the value of Γ_1 was in most cases smaller than 2 meV, so that a fit of acceptable quality could be performed with Eq. (18) for $\Gamma_1=0$, i.e., with only two parameters Γ_0 and Θ . Values of $\Gamma_1 \neq 0$ obtained from fits to experimental data may correspond to other broadening mechanisms (e.g., electron-electron interaction, impurities, surface scattering). The parameters Γ_0 and Θ obtained from the fits of all the calculated initial states of the valence and conduction bands of Si and Ge are given in Table I. Note that Γ_0 gives the broadening at $T=0$. The average phonon frequency indicates how large the contribution of the acoustic phonons to the broadening is. For example, for the VB states of Si along the Δ direction (see Fig. 2) this contribution is small. This results in a high value for Θ (540 K). In the case of the corresponding CB states, however, the smaller average frequency of $\Theta \approx 350$ K indicates a larger acoustic phonon contribution which can be clearly seen from Fig. 3. From the fit parameters Γ_0 and Θ it is possible to determine an average electron-phonon deformation potential \bar{D} by performing an average over the contributions to $\Gamma_{kn}(T)$ of the whole BZ and over the phonon branches j . Thus, from Eq. (10) we obtain

$$\Gamma_{kn}(T) = \left\langle \frac{\partial \Gamma_{kn}}{\partial n} \right\rangle_{\text{BZ}} \left[n(\Theta) + \frac{1}{2} \right], \quad (19)$$

with Θ the temperature corresponding to the average phonon energy. We define the averaged electron-phonon deformation potential \bar{D} as

$$\begin{aligned} \left\langle \frac{\partial \Gamma_{kn}}{\partial n} \right\rangle_{\text{BZ}} &= 6\pi [\bar{D}(\mathbf{k}, n)]^2 \left\langle \frac{\langle u^2 \rangle}{a^2} \right\rangle N_e(\mathbf{k}, n), \\ &= 6 \frac{\pi \hbar}{M \bar{\omega} a^2} [\bar{D}(\mathbf{k}, n)]^2 N_e(\mathbf{k}, n), \end{aligned} \quad (20)$$

where $\langle u^2 \rangle$ is the averaged squared phonon amplitude, a the lattice constant, $\bar{\omega}$ an average phonon frequency, which, in the spirit of Eq. (18), should be set equal to $k_B \Theta / \hbar$, and $N_e(\mathbf{k}, n)$ the electronic density of states at the energy of the initial state (\mathbf{k}, n) . The factor of 6 in Eq. (20) takes into account the six phonon branches giving contributions to the broadening. With this definition we can write Eq. (19) in the following way:

$$\Gamma_{kn}(T) = 6\pi \frac{\hbar}{M \bar{\omega} a^2} [\bar{D}(\mathbf{k}, n)]^2 N_e(\mathbf{k}, n) \left[\frac{1}{e^{\Theta/T} - 1} + \frac{1}{2} \right]. \quad (21)$$

Taking $\bar{\omega} = k_B \Theta / \hbar$, the deformation potential \bar{D} is determined by the fit parameters Γ_0 and Θ from Eq. (18):

$$\bar{D}(\mathbf{k}, n) = \left[\frac{M a^2 k_B}{3\pi \hbar^2} \frac{\Gamma_0 \Theta}{N_e(\mathbf{k}, n)} \right]^{1/2}. \quad (22)$$

For the electronic density of states at the energy of the in-

TABLE I. Values of the parameters Γ_0 and Θ obtained by fitting the calculated Lorentzian broadening parameter Γ versus temperature T to the equation $\Gamma(T) = \Gamma_0 [1 + 2/(e^{\Theta/T} - 1)]$ for several electronic states of the valence and conduction band of Si and Ge. Furthermore, the electronic density of states N_e are listed, calculated with the tetrahedron method for the electron energies. \bar{D} is an averaged electron-phonon deformation potential, defined in Eq. (20).

	Si				Ge			
	Γ_0 (meV)	Θ (K)	N_e ($1 \text{ eV}^{-1} \text{ atom}^{-1}$)	\bar{D} (eV)	Γ_0 (meV)	Θ (K)	N_e ($1 \text{ eV}^{-1} \text{ atom}^{-1}$)	\bar{D} (eV)
	Valence band							
$\Gamma_{25'}$	0							
0.25L	10.88(14)	620(9)	0.089	11.7	8.31(7)	390(4)	0.097	13.1
0.50L	25.82(28)	583(7)	0.230	10.9	21.43(19)	358(3)	0.252	12.5
0.75L	34.07(35)	559(6)	0.351	9.9	29.42(26)	343(3)	0.418	11.1
L_3	42.18(43)	554(7)	0.484	9.4	36.73(34)	337(3)	0.591	10.3
0.25X	25.83(28)	583(7)	0.254	10.4	19.30(20)	360(4)	0.085	20.4
0.50X	43.78(47)	514(6)	0.616	8.1	37.02(38)	317(3)	0.252	15.4
0.75X	37.91(48)	471(6)	0.722	6.7	28.87(38)	285(4)	0.644	8.1
X_4	31.59(54)	436(8)	0.712	5.9	24.79(41)	274(5)	0.713	7.0
$(2\pi/a)(0.9, 0.1, 0.1)$	33.66(53)	446(8)	0.738	6.1				
$(2\pi/a)(0.75, 0.25, 0.25)$					31.87(38)	299(4)	0.767	8.0
	Conduction band							
Γ_{15}	23.69(32)	525(8)	0.468	7.0	15.63(44)	237(7)	0.406	6.8
$\Gamma_{2'}$	25.13(28)	223(3)	0.856	3.4	1.459(1)	320(2)	0.343	2.6
0.25L	27.71(60)	418(10)	0.690	5.5	12.94(27)	230(5)	0.587	5.1
0.50L	20.17(99)	405(21)	0.624	4.9	5.84(10)	252(5)	0.278	5.2
0.75L	10.56(20)	398(8)	0.370	4.5	0.54(1)	245(6)	0.037	4.3
L_1	8.91(17)	389(8)	0.315	4.5	0			
0.25X	29.35(43)	484(8)	0.696	6.1	23.08(55)	244(6)	0.710	6.4
0.50X	9.40(15)	492(9)	0.208	6.3	7.99(17)	258(6)	0.305	5.9
0.75X	1.004(3)	393(15)	0.012	7.7	0.14(1)	229(8)	0.008	4.5
X_1	0.32(1)	414(17)	0.022	3.3	1.179(4)	251(8)	0.075	4.5
$(2\pi/a)(0.9, 0.1, 0.1)$	3.19(6)	480(10)	0.085	5.7				
$(2\pi/a)(0.75, 0.25, 0.25)$					12.94(36)	234(7)	0.498	5.6

initial state we took the values obtained with the tetrahedron method²⁴ for the electrons. These values of $N_e(\mathbf{k}, n)$ as well as those for the average electron-phonon deformation potential $\bar{D}(\mathbf{k}, n)$ are listed in Table I for electronic states along the Λ and Δ lines in the BZ of Si and Ge.

We should mention that for semiconducting lead chalcogenides a detailed study of the broadening of critical points, as obtained by photoemission spectra, has been performed.²⁷ From the linear dependence of the broadenings with temperature a similarly defined averaged deformation potential has been determined to be $\bar{D} = 30$ eV for PbS and $\bar{D} = 23$ eV for PbSe, values which when divided by a factor of $\sqrt{6}$ (resulting from a different definition of \bar{D}) are similar to those obtained here for the VB of Si and Ge.

V. BROADENING OF CRITICAL POINTS

We now combine the results of the preceding section for the broadening of the valence- and conduction-band states in order to obtain the temperature-dependent broadening of the critical points, $\Gamma = \Gamma_{\text{VB}} + \Gamma_{\text{CB}}$. The results are compared with data measured by spectroscopic ellipsometry, as far as available

A. E_1 critical points

The lifetime broadening of the E_1 transitions is taken to be the average of those for $\mathbf{k} = (\pi/2a)(1, 1, 1)$, $\mathbf{k} = (3\pi/4a)(1, 1, 1)$, and $\mathbf{k} = (\pi/a)(1, 1, 1)$. Figure 8(a) shows the resulting broadening for Si and Fig. 8(b) shows that for Ge (solid lines), together with the experimental data. The parameters for the fits of the calculated data to Eq. (18) for $\Gamma_1 = 0$, as well as the parameters from the fit of the experimental data, are given in Table II. In the case of Si, the E'_0 gap is nearly degenerate with the E_1 gap at room temperature, so that it is difficult to distinguish these two contributions. However, at 10 K there seems to be a separation of about 100 meV (measured by electroreflectance²⁸). The E_1 and E'_0 transitions have also been resolved with ellipsometry,⁷ thus obtaining data for the broadening of the E_1 as well as for the E'_0 gap up to 280 K. The corresponding experimental points⁷ are shown in Fig. 8(a) as open squares (Γ_{E_1}) and open triangles ($\Gamma_{E'_0}$). At higher temperatures ($T > 280$ K) the points obtained from the fits (solid squares) represent a mixture between the two contributions. Our band-structure calculations do not take into account in the spin-orbit splitting,

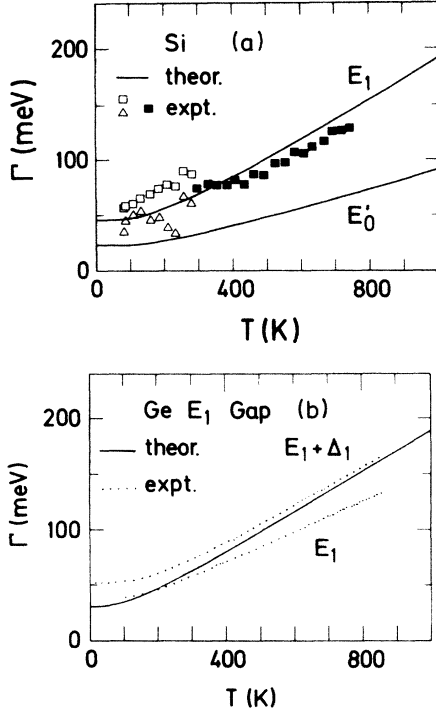


FIG. 8. Lifetime broadening of the E_1 gap for (a) Si and (b) Ge and of the E'_0 gap for Si (a), with energy nearly degenerate with E_1 . Solid lines: calculated phonon-induced broadening. (a) Experimental points: \triangle and \square , two critical points in the E_1 region. \blacksquare , one CP in the E_1 region. (b) Dotted lines are fits to the experimental data of the E_1 and $E_1 + \Delta_1$ transitions.

which for the E_1 transitions of Si is nevertheless about 30 meV and thus smaller than the lifetime broadening.

For Ge, however, the spin-orbit splitting Δ_1 can be clearly resolved in ellipsometric and other spectra ($\Delta_1 = 187$ meV, Ref. 4). The dotted lines in Fig. 8(b) indicate the fits to the experimental data for the broadenings

of E_1 and $E_1 + \Delta_1$, the one for $E_1 + \Delta_1$ showing higher values because of the higher density of states for the lower VB split by spin-orbit interaction. The calculated theoretical solid line, which should thus be interpreted as a mean value of E_1 and $E_1 + \Delta_1$, shows good agreement with the experimental data.

B. Direct gaps E_0 and E'_0

The parameters describing the lifetime broadening of the direct gaps E_0 and E'_0 with the help of Eq. (18) (for $\Gamma_1 = 0$) are also given in Table II. As already mentioned in the preceding section, the lowest direct transition in Si, E'_0 , is nearly degenerate with the E_1 critical point. At low temperatures, however, we succeeded in separating the E'_0 from the E_1 transitions. The experimental points (open triangles) are shown in Fig. 8(a), together with the theoretical curve. Because of the low strength of the E'_0 transitions, the values for $\Gamma_{E'_0}$ scatter and seem to be systematically slightly larger than the calculated ones.

The " E_0 " transitions in Si, from the $\Gamma_{25'}$ VB to the $\Gamma_{2'}$ CB states (4.2 eV, Ref. 29), are very weak and, to our knowledge, no experimental data for the temperature dependence of their broadening parameter are available. The same is true for the E'_0 transitions of Ge, taking place between the $\Gamma_{25'}$ VB state and the Γ_{15} CB state. Here because of the spin-orbit splitting of the VB states, Δ_0 , as well as of the CB states, Δ'_0 , one obtains a rather broad structure in the spectrum of the dielectric constant arising from the E'_0 and $E'_0 + \Delta'_0$ CP's.⁴ It was not possible to resolve these points reliably, especially at high temperature.⁴ The lowest direct transition of Ge (E_0) is strongly affected by exciton interaction. Only the $\Gamma_{2'}$ CB state broadens with increasing temperature, within the approximation used. For this broadening we found rather small values (see Table I), due, in part, to the small density of electronic states.

TABLE II. Values of the parameters Γ_0 and Θ obtained by fitting the calculated broadening parameter Γ versus temperature T to the equation $\Gamma(T) = \Gamma_0 [1 + 2/(e^{\Theta/T} - 1)]$, labeled as theory. For comparison, the fit parameters for the experimental data are listed. For the E_2 transition different parameters are obtained for fitting the critical point line shape with a 1D or 2D model.

	Si		Γ_1 (meV)	Ge		Γ_1 (meV)
	Γ_0 (meV)	Θ (K)		Γ_0 (meV)	Θ (K)	
E_0 gap theory	23.7(3)	525(8)		1.459(1)	320(2)	
E'_0 gap theory	25.1(3)	223(3)		15.6(4)	237(7)	
E_1 gap theory	47.4(8)	505(10)		31.3(3)	336(4)	
E_1 gap experiment	59 ^a	743 ^a		25 ^b	376 ^b	12 ^b
				43 ^c	484 ^c	9 ^c
E_2 gap theory	36.8(6)	449(8)		45.0(7)	278(5)	
E_2 gap experiment 1D	16 ^d	163 ^d	76 ^d	72 ^e	429 ^e	31 ^e
E_2 gap experiment 2D	18 ^d	261 ^d	59 ^d	69 ^e	499 ^e	8 ^e

^a Reference 7, data for the mixture of E_1 and E'_0 contributions fitted from 280 to 750 K to $\Gamma(T) = \Gamma_0 [1 + 2/(e^{\Theta/T} - 1)]$.

^b Reference 4, experimental data for the E_1 transition, fitted with Eq. (18).

^c Reference 4, experimental data for the $E_1 + \Delta_1$ transition, fitted with Eq. (18).

^d Reference 7, experimental data fitted with Eq. (18).

^e Reference 4, experimental data fitted with Eq. (18).

C. E_2 critical points

The origin of the strong E_2 structure in the optical spectra is not well defined. It has been attributed to transitions in several regions of the BZ, thus rather poorly localized in \mathbf{k} space. To determine the broadening we have used the transitions at the point $(2\pi/a)(0.9,0.1,0.1)$ for Si and $(2\pi/a)(0.75,0.25,0.25)$ for Ge as representative.²⁶ Fitting the calculated temperature-dependent broadening to Eq. (18) (with $\Gamma_1=0$) yields the parameters given in Table II.

In Fig. 9 we show the comparison between theoretical and experimental data, the last ones obtained again from ellipsometrical measurements, by fitting the second derivative of the dielectric function with respect to the photon energy to theoretical CP line shapes.^{30,31} In the case of the E_2 CP it is possible to fit its line shape with models having different dimensionality. For Si at room temperature the fits were performed with a one-dimensional (1D) maximum for E_2 .³² However, in doing the temperature-dependent measurements of the dielectric function of Ge, InSb, and α -Sn,⁴⁻⁶ it appeared that a two-dimensional (2D) CP is the best representation of this

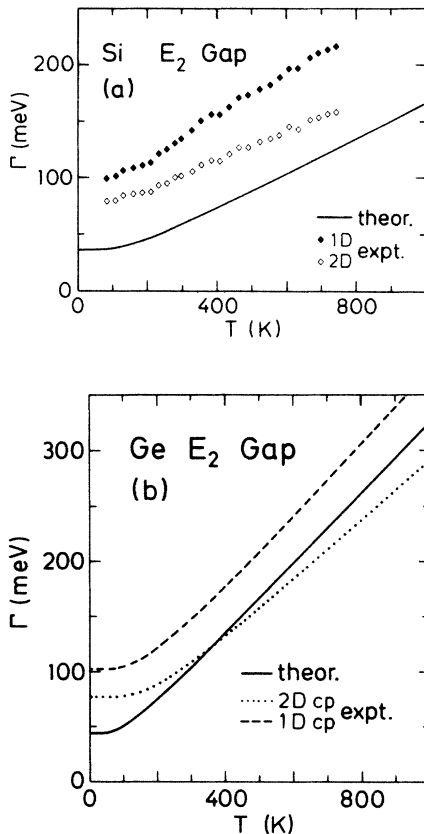


FIG. 9. Lifetime broadening of the E_2 gap for (a) Si and (b) Ge. Solid lines: phonon-induced broadening calculated for a representative point of the E_2 transitions. Experimental data, fitted with a 1D line shape, are shown by the solid points for (a) Si and the dashed line for (b) Ge, the data fitted with a 2D line shape are indicated by open points for (a) Si and by a dotted line for Ge (b).

structure over the entire temperature range.⁴⁻⁶ In Fig. 9 we have plotted for comparison the experimental data obtained by fitting a 1D [solid points for Si,⁷ Fig. 9(a); dashed line for Ge,⁴ Fig. 9(b)]; and a 2D line shape [open points for Si,⁷ Fig. 9(a); dotted line for Ge,⁴ Fig. 9(b)], together with the calculated curve for the broadening parameter of E_2 . The experimental data fitted with a 2D line shape give smaller broadening parameters, lying closer to the calculated ones. The facts suggest that the E_2 transitions can, indeed, be better represented by two-dimensional critical points. However, the local pseudopotential band structure used in our calculations underestimates the E_2 CP energies by about 10%. A higher CP energy would lead to a higher electronic density of states and thus to higher values for the broadening parameters.

VI. DISCUSSION

To calculate the broadenings, only electronic states lying in the same energy region as the initial state are taken into account [see Eq. (11)]. Thus the method is sensitive to the details of the band-structure model and to the accuracy of the interpolation between the mesh of little tetrahedra used to perform the BZ integration. We have used a simple local pseudopotential band structure without spin-orbit splittings which underestimates the gap energy near the X point by about 10%. The BZ was chosen to be divided into 228 little tetrahedra in the irreducible $\frac{1}{48}$ th wedge of the BZ, corresponding to eight intervals lying between the Γ and the X point. The tetrahedron method performs linear interpolations between neighboring points, so that band bendings are flattened. However, this effect should lead only to small errors in comparison with inaccuracies of the electron energies inherent to the band-structure calculation.

Our calculation assumes negligibly small phonon energies (as compared with electronic energies). A more general theory in which this restriction is lifted has been given by Allen.¹⁵ It is based on Feynman-Dyson perturbation theory instead of the Rayleigh-Schrödinger version used here. In the Feynman-Dyson expressions for the electron self-energies the complex perturbed energies $\epsilon_{\mathbf{k}n} + \Delta\epsilon_{\mathbf{k}n} + i\Gamma_{\mathbf{k}n}$ appear in the energy denominators, together with the phonon frequencies. The latter appear with different signs in the expressions which correspond to phonon absorption and phonon emission. The changes induced by the finite phonon frequencies should thus nearly cancel at high temperatures except near a band edge where the density of electronic states exhibits a strong singularity.

The energy $\Delta\epsilon_{\mathbf{k}n}$ leads to relative shifts of the band structure and thus to changes in the density of states N_e with increasing temperature. This should be important if different parts of the band structure having nearly the same energy shift with temperature at different rates (e.g., the Γ_2' and the L_1 CB states of Ge. The difference in their shifts at 800 K is 120 meV¹⁹).

We can estimate the error due to neglecting the difference of perturbed and unperturbed electron energy and the phonon energy by examining the corresponding change in the electronic density of states:

$$\Delta\Gamma/\Gamma \cong (dN_e/dE)\Delta E/N_e, \quad (23)$$

where ΔE represents the relative energy shift plus or minus the phonon energy. Typical values for dN_e/dE are for both Si and Ge $1/(eV^2 \text{ atom})$. From Eq. (23) it is obvious that small values for N_e such as occur near the VB maximum and the CB minimum will produce particularly large errors in $\Gamma(T)$. However, the electronic states contributing to most of the interband critical points lie in regions with larger density of states, a fact which reduces the error. Taking into account these corrections and using a more realistic band structure would strongly increase the computer time required for the calculation. [Our calculation of the broadening of the VB state at the L point of Si took already more than 2 h of central processing unit (CPU) time on a Honeywell-Bull 60-80P computer.]

It should also be possible, in principle, to calculate the expression for $\partial\Gamma_{\mathbf{k}n}/\partial n_{Qj}$ [Eq. (13)], by replacing the δ function $\delta(\epsilon_{\mathbf{k}n} - \epsilon_{\mathbf{k}+Q,n'})$ by its representation:

$$\delta(x) = \lim_{\Delta \rightarrow 0^+} \left[\frac{1}{\pi} \frac{\Delta}{x^2 + \Delta^2} \right], \quad (24)$$

and performing only one integration with the standard tetrahedron method. The corresponding real part would then be the principal value of $1/x$:

$$P \int \frac{1}{x} dx = \lim_{\Delta \rightarrow 0^+} \frac{x}{x^2 + \Delta^2}. \quad (25)$$

The calculations of the temperature shift¹⁷⁻¹⁹ have been performed with expressions corresponding to Eq. (25), using a broadening of $\Delta=0.01$ Ry.¹⁷ This large value was chosen so as to smooth the noise arising from the finite-mesh size of the calculation. For a good representation of the δ function [Eq. (24)], however, it is necessary to choose a much smaller value of Δ . By doing so, because of our coarse mesh, energy bands crossing the energy of the initial state $\epsilon_{\mathbf{k}n}$ may be incorrectly taken into account

if their energies at neighboring mesh points are very different from each other. To circumvent this problem, we used the tetrahedron method in the form of Ref. 23 with linear interpolation of the values of the mesh points. The results obtained and the comparison with experimental data are quite rewarding and justify the adequacy of the procedure employed.

VII. CONCLUSIONS

We have calculated the lifetime broadening of electronic states induced by phonons and its temperature dependence in germanium and silicon. The results show good agreement with experimental data obtained by means of spectroscopic ellipsometry. Our model is based on a perturbative calculation of the imaginary part of the self-energy to second order in atomic displacements.

The calculated temperature dependence of the broadenings can be fitted with a phenomenological expression based on Bose-Einstein factors and containing two adjustable parameters, one of them an average phonon temperature. The calculations were performed for points along the Λ and Δ lines, and a few other points of the BZ, from which the broadenings of the E_0 , E'_0 , E_1 , and E_2 critical points could be determined. The averaged frequencies of the phonons involved turned out to be different for VB and CB states at the same point of the BZ. An averaged electron-phonon deformation potential was defined to describe the strength of the coupling.

ACKNOWLEDGMENTS

Thanks are due to L. Viña and H. Weiler for a number of discussions and to C. K. Kim for a critical reading of the manuscript. One of us (P.B.A.) is grateful to the Alexander von Humboldt Foundation for support and also acknowledges support from the U.S. National Science Foundation Grant No. DMR-84-20308.

*Permanent address: Department of Physics, State University of New York at Stony Brook, Stony Brook, NY 11794.

¹D. E. Aspnes, Opt. Commun. **8**, 222 (1973); D. E. Aspnes and A. A. Studna, Appl. Opt. **14**, 220 (1975).

²See, for instance, *Landolt-Börnstein Tables: Semiconductors*, edited by O. Madelung, M. Schulz, and H. Weiss (Springer, Heidelberg, 1982), Vol. 17. For details of the notation used to represent optical interband critical points, see M. Cardona, in *Atomic Structure and Properties of Solids*, edited by E. Burstein (Academic, New York, 1972), p. 514.

³G. E. Jellison, Jr. and F. A. Modine, Phys. Rev. B **27**, 7466 (1983).

⁴L. Viña, S. Logothetidis, and M. Cardona, Phys. Rev. B **30**, 1979 (1984).

⁵S. Logothetidis, L. Viña, and M. Cardona, Phys. Rev. B **31**, 947 (1985).

⁶L. Viña, H. Höchst, and M. Cardona, Phys. Rev. B **31**, 958 (1985).

⁷P. Lautenschlager, L. Viña, and M. Cardona (unpublished).

⁸See, for instance, W. Hanke, N. Meskini, and H. Weiler, in *Electronic Structure, Dynamics, and Quantum Structural*

Properties of Condensed Matter, edited by J. T. Devreese and P. van Camp (Plenum, New York, 1985).

⁹M. L. Cohen and D. J. Chadi, in *Semiconductor Handbook*, edited by M. Balkanski (North-Holland, Amsterdam, 1980), Vol. 2, Chap. 4B.

¹⁰E. Antoncik, Czech. J. Phys. **5**, 449 (1955).

¹¹H. Y. Fan, Phys. Rev. **82**, 900 (1951).

¹²M. L. Cohen, Phys. Rev. **128**, 131 (1962).

¹³P. B. Allen and V. Heine, J. Phys. C **9**, 2305 (1976).

¹⁴M. Schlüter, G. Martinez, and M. L. Cohen, Phys. Rev. B **12**, 650 (1975).

¹⁵P. B. Allen, Phys. Rev. B **18**, 5217 (1978); B. Chakraborty and P. B. Allen, *ibid.* **18**, 5225 (1978).

¹⁶S. K. Sinha, Phys. Rev. **169**, 477 (1968).

¹⁷P. B. Allen and M. Cardona, Phys. Rev. B **23**, 1495 (1981); **24**, 7479 (1981).

¹⁸P. B. Allen and M. Cardona, Phys. Rev. B **27**, 4760 (1983).

¹⁹P. Lautenschlager, P. B. Allen, and M. Cardona, Phys. Rev. B **31**, 2163 (1985).

²⁰P. Lawaetz, The Influence of Holes on the Phonon Spectrum of Semiconductors Technical, D. Sc. thesis, Technical Univer-

- sity of Denmark, 1978 (unpublished).
- ²¹M. L. Cohen and T. K. Bergstresser, *Phys. Rev.* **141**, 789 (1966).
- ²²W. Weber, *Phys. Rev. B* **15**, 4789 (1977).
- ²³P. B. Allen, *Phys. Status Solidi B* **120**, 529 (1983).
- ²⁴G. Lehmann and M. Taut, *Phys. Status Solidi B* **54**, 469 (1972); **57**, 815 (1973).
- ²⁵O. H. Nielsen and W. Weber, *Comput. Phys. Commun.* **18**, 101 (1979).
- ²⁶J. R. Chelikowsky and M. L. Cohen, *Phys. Rev. B* **14**, 556 (1976); *Phys. Rev. Lett.* **31**, 1582 (1973).
- ²⁷T. Grandke, M. Cardona, and L. Ley, *Solid State Commun.* **32**, 353 (1979).
- ²⁸A. Daunois and D. E. Aspnes, *Phys. Rev. B* **18**, 1824 (1978).
- ²⁹D. E. Aspnes and A. A. Studna, *Solid State Commun.* **11**, 1375 (1972).
- ³⁰M. Cardona, *Modulation Spectroscopy*, Suppl. 11 of *Solid State Physics* (Academic, New York, 1969).
- ³¹Y. Toyozawa, M. Inoue, T. Inui, M. Okazaki, and E. Hanamura, *J. Phys. Soc. Jpn. Suppl.* **21**, 133 (1967).
- ³²L. Viña and M. Cardona, *Phys. Rev. B* **29**, 6739 (1984).